

Optical microscopy of electronic and structural properties of epitaxial laterally overgrown GaN

A. Kaschner,^{a)} A. Hoffmann, and C. Thomsen

Institut für Festkörperphysik, Technische Universität Berlin, Hardenbergstrasse 36, 10623 Berlin, Germany

F. Bertram, T. Riemann, and J. Christen

Institut für Experimentelle Physik, Otto-von-Guericke-Universität, PO Box 4120, 39016 Magdeburg, Germany

K. Hiramatsu

Department of Electrical and Electronic Engineering, Mie University, Mie 514-8507, Japan

T. Shibata and N. Sawaki

Department of Electronics, Nagoya University, Nagoya 464-01, Japan

(Received 12 January 1999; accepted for publication 17 March 1999)

Local strain relaxation as well as inhomogeneous impurity incorporation in epitaxial laterally overgrown GaN (ELOG) structures is microscopically characterized using spectrally resolved scanning cathodoluminescence (CL) and micro-Raman spectroscopy. We correlate the different CL emission spectra with results of spatially resolved Raman-scattering experiments sensing the local strain and free-carrier concentration. © 1999 American Institute of Physics. [S0003-6951(99)03220-9]

Gallium nitride and its related ternary alloys have been evolving to become the most prosperous material for light emitting diodes and laser diodes in the blue spectral range.¹ Recently, laser diodes with an estimated lifetime of more than 10^4 h were reported.² One major advancement for commercial application was the introduction of the epitaxial lateral overgrowth (ELO) technique for the wide-gap III-V materials.³⁻⁶ This method is effective in reducing dislocation density in GaAs and InP layers on silicon substrates.⁷⁻⁹ In GaN the dislocation density is reduced by 3-4 orders of magnitude from that of heteroepitaxial GaN layers grown on sapphire substrates ($\sim 10^{10}$ cm⁻²).^{10,11} Some authors report on improvements of the defect structure of ELOG samples observed in transmission electron microscopy,¹¹⁻¹³ and it was shown that lateral overgrowth leads directly to improved electrical properties of GaN *p-n* junctions.¹⁴ Basic optical characterization was also performed.¹⁵⁻¹⁷ A correlation of the optical properties with local strain and free-carrier concentrations of ELOG structures oriented along the $\langle 11\bar{2}0 \rangle$ direction has been put forward in Ref. 18.

The ELOG sample investigated here is a 3- μ m-thick GaN layer grown by metalorganic vapor phase epitaxy (MOVPE) on a (0001) sapphire substrate and patterned with a 120-nm-thick SiO₂ mask of parallel stripes oriented along the $\langle 1\bar{1}00 \rangle$ direction. The width of the openings and the stripes are 10 μ m each. This structure was subsequently overgrown with a 50- μ m-thick GaN layer deposited by hydride vapor phase epitaxy (HVPE) through the windows in the SiO₂ mask on the underlying MOVPE GaN layer. The cathodoluminescence (CL) measurements were performed at 5 K. A spatial resolution better than 40 nm is achieved. Details of this technique have been described elsewhere.¹⁹ Micro-Raman (μ -Raman) measurements were carried out in backscattering geometry. With the 488 nm line of an Ar⁺/Kr⁺ gas laser for excitation, out-frequencies have an

accuracy of 0.1 cm⁻¹. The lateral spatial resolution is 0.7 μ m.

In Fig. 1(a) a secondary electron image of the sample cross section is depicted together with the corresponding CLWI [Fig. 1(b)]. Thus, both the cleaved cross section as well as part of the sample surface are visible. One can see well the overgrown region above the SiO₂ mask and the area of the coherent growth among the stripes. The latter forms a uniform monochromatic rectangle up to the surface where the local CL spectra are dominated by the sharp excitonic luminescence at 357.6 nm.

In Fig. 2 a magnified CLWI (a) is shown together with an integral spectrum (b) and a set of local CL spectra (c-h). The local CL spectrum in this area (c) exhibits sharp excitonic luminescence. The dominating luminescence is the neutral-donor-bound exciton emission (D_1^0, X) at 357.6 nm [local spectrum Fig. 2(e)]. The two neighboring peaks with lower intensities at 357.2 nm and 358.0 nm are assigned as free-exciton transition (X) and (D_2^0, X) emission, respectively.²⁰ In regions that appear yellow in the CLWI the (D_1^0, X) and the (D_2^0, X) transitions have about the same intensity, indicating a higher local concentration of the D_2 do-

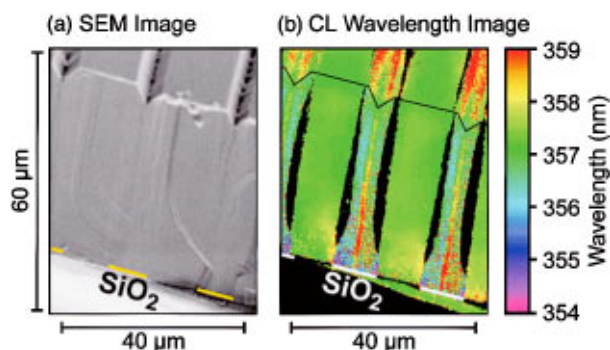


FIG. 1. SEM image (a) and a CLWI (b) of the sample cross section under investigation measured under 45° observation. Areas of vanishing CL intensity are blackened in the CLWI.

^{a)}Electronic mail: kaschner@physik.tu-berlin.de

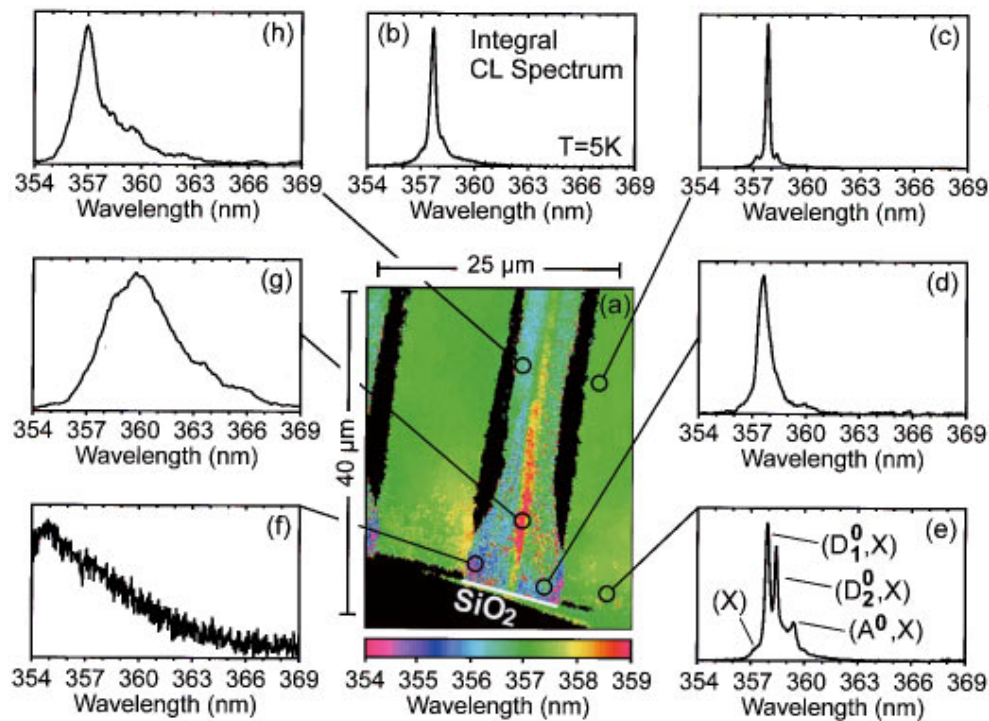


FIG. 2. CL wavelength image (a), local CL spectra (c)–(h) of different regions, and an integral spectrum (b).

nor. In Fig. 2(e) a further line becomes visible which is assigned to emission from neutral-acceptor-bound exciton (A^0, X).

The overgrowth region is dominated by a strongly redshifted luminescence in the coalescence region centered 7 μm above the SiO₂ stripe. This redshift [Fig. 2(g)] is explained by a high impurity incorporation at the merging crystal planes and resulting voids. A broad and blueshifted spectrum from the edges of the SiO₂ stripes is depicted in Fig. 2(f). Here the free-electron concentration becomes so large that the recombination process is dominated by an electron–hole plasma rather than by excitonic emission. No luminescence is detected in areas which are masked out black even in the spectral region of the yellow luminescence. In this region nonradiative processes dominate over all radiative processes since the density of structural defects is very high as confirmed by transmission electron microscopy.²¹

In order to understand the spatial dependence of the luminescence we performed μ-Raman scattering experiments along a line from the substrate interface to the sample’s surface. Figure 3 shows Raman spectra at different distances from the interface in the overgrown region. At a distance of 1 μm, i.e., within the MOVPE GaN buffer layer, the Fröhlich-allowed $E_1(LO)$ mode can be observed together with the $A_1(TO)$ and E_2 mode as well as structures originating from second-order Raman scattering.²² Further away from the interface towards the surface the $E_1(LO)$ mode vanishes and LPP modes appear. From the LPP mode position we deduced the free-electron concentration.²³ Additionally, a peak marked by an asterisk appears which is typical for GaN with a large free-carrier concentration.

The upper part of Fig. 4 shows that the free-carrier concentration in the overgrown region outside the buffer layer decreases up to a distance of 10 μm from the substrate. We believe that the free electrons in the part right above the

mask mainly stem from indiffused silicon or oxygen atoms creating shallow donor levels. From 10 to 40 μm from the interface the free-carrier concentration remains constant at $8.7 \times 10^{18} \text{ cm}^{-3}$. This is where we observe the redshifted luminescence in the CL spectra. It is possible that either intrinsic or impurity related donors are associated with the structurally defective area in the coalescence region giving rise to a high free-electron concentration. Starting at 40 μm above the substrate the free-electron concentrations drop off and reach the value determined for the coherently grown region

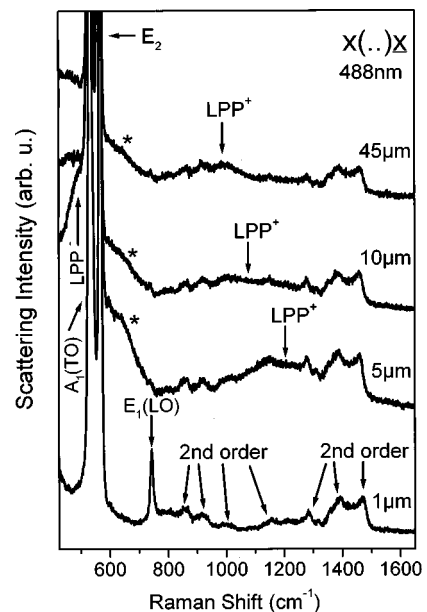


FIG. 3. Room-temperature Raman spectra taken at various distances from the substrate interface in the overgrown region. LPP modes appear outside the 3 μm GaN buffer layer accompanied by the mode at around 650 cm⁻¹ (marked by an asterisk) indicating a high free-carrier concentration.

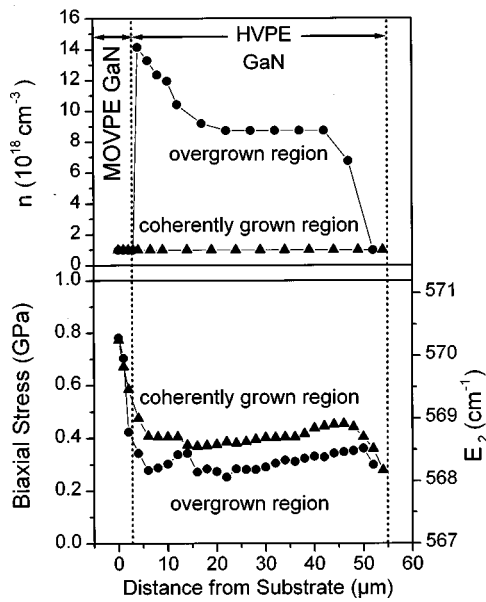


FIG. 4. Free-carrier concentration as determined from the LPP mode position and E_2 line position indicating the biaxial compressive stress vs distance from the substrate interface in the overgrown region as well as in the coherently grown area.

right below the surface. The Raman spectra from the region of coherent growth do not exhibit LPP modes, therefore we conclude for all distances $n < 1 \times 10^{18} \text{ cm}^{-3}$ which is the detection limit of this method. However, the actual concentration may be much smaller.

The lower part of Fig. 4 shows the dependence of the E_2 position, which is a measure of the biaxial stress in the material, as a function of distance from the interface. The major part of stress relaxation takes place in the $3 \mu\text{m}$ MOVPE GaN layer. When approaching the surface a second step in stress relaxation occurs and the E_2 frequency (568 cm^{-1}) almost reaches the value known for completely relaxed GaN (567 cm^{-1}). As reported in Ref. 18 we also observe a faster stress relaxation in the ELOG region as compared to the coherently grown domains which is probably due to a higher concentration of structural defects.

Summarizing the CL and Raman-scattering results we find that the strong incorporation of defects in the coalescence area is accompanied by a high free-electron concentration. In contrast the coherently grown region exhibits a free-carrier concentration below our detection limit and shows a rectangle of sharply defined excitonic luminescence up to the surface. For the ELOG sample discussed in Ref. 18 having the SiO_2 stripes in $\langle 11\bar{2}0 \rangle$ direction a triangle only $14 \mu\text{m}$ in height appears with a sharp excitonic luminescence. A jump in free-carrier concentration occurs on top of this triangle. These observations are in perfect agreement with the growth model of ELO GaN. In Ref. 24 it is outlined that the vertical growth rates decrease, while the lateral overgrowth rates increase as the mask stripe orientation changes from $\langle 11\bar{2}0 \rangle$ to $\langle 1\bar{1}00 \rangle$. Therefore the triangle appearing for the sample with the masks along $\langle 11\bar{2}0 \rangle$ direction extends to form a rectangle for the $\langle 1\bar{1}00 \rangle$ ELOG structure. In both structures we find very poor crystalline and optical properties in the overgrown region, especially in the coalescence region.

An ELOG structure with SiO_2 mask orientation along

$\langle 1\bar{1}00 \rangle$ direction is comprehensively micro-optically characterized. The coherently grown regions show excitonic luminescence and low free-carrier concentration evidenced by μ -Raman spectroscopy. In contrast the overgrown region is dominated by a blueshifted CL emission which can be attributed to a strong impurity incorporation. The free-carrier concentration starting at a value of $1.4 \times 10^{19} \text{ cm}^{-3}$ right outside the buffer layer decreases up to a distance of $10 \mu\text{m}$ away from the substrate and then remains constant up to $40 \mu\text{m}$. We believe that in the first part the indiffusion of silicon and oxygen and in the second part structural defects are responsible for the high concentration of free electrons. The relaxation of the biaxial compressive stress due to the large lattice mismatch between GaN and the sapphire substrate mostly occurs in the $3 \mu\text{m}$ MOVPE GaN. Extrinsic luminescence at $\lambda > 360 \text{ nm}$ dominates the CL from the coalescence region above the center of the SiO_2 masks indicating strong impurity accumulation in this structurally defective region.

A.K. is supported by an E.-v.-Siemens-scholarship.

- ¹For a review, see S. Nakamura and G. Fasol, *The Blue Laser Diode* (Springer, Heidelberg, 1997).
- ²S. Nakamura, M. Senoh, S. Nagahama, N. Iwasa, T. Yamada, T. Matushita, H. Kiyoku, Y. Sugimoto, T. Kozaki, H. Umemoto, M. Sano, and K. Chocho, *Jpn. J. Appl. Phys., Part 2* **36**, L1568 (1997).
- ³Y. Kato, S. Kitamura, K. Hiramatsu, and N. Sawaki, *J. Cryst. Growth* **144**, 133 (1994).
- ⁴D. Kapolnek, S. Keller, R. Vetry, R. D. Underwood, P. Kozodoy, S. P. Den Baars, and U. K. Mishra, *Appl. Phys. Lett.* **71**, 1204 (1997).
- ⁵T. S. Zheleva, O.-H. Nam, M. D. Bremser, and R. F. Davis, *Appl. Phys. Lett.* **71**, 2472 (1997).
- ⁶O.-H. Nam, M. D. Bremser, T. S. Zheleva, and R. F. Davis, *Appl. Phys. Lett.* **71**, 2638 (1997).
- ⁷D. Pribat, B. Gerad, M. Dupuy, and P. Legagneux, *Appl. Phys. Lett.* **60**, 2144 (1992).
- ⁸S. F. Fang, K. Adomi, S. Iyer, H. Morkoç, H. Zabel, C. Choi, and N. Otsuka, *Appl. Phys. Lett.* **68**, R31 (1992).
- ⁹S. D. Lester, F. A. Ponce, M. G. Craford, and D. A. Steigerwald, *Appl. Phys. Lett.* **66**, 1249 (1996).
- ¹⁰A. Usui, H. Sunakawa, A. Sakai, and A. Yamaguchi, *Jpn. J. Appl. Phys., Part 2* **36**, L899 (1997).
- ¹¹H. Marchand, X. H. Wu, J. P. Ibbetson, P. T. Fini, P. Kozodoy, S. Keller, J. S. Speck, S. P. Den Baars, and U. K. Mishra, *Appl. Phys. Lett.* **73**, 747 (1998).
- ¹²A. Sakai, H. Sunakawa, and A. Usui, *Appl. Phys. Lett.* **71**, 2259 (1997).
- ¹³A. Sakai, H. Sunakawa, and A. Usui, *Appl. Phys. Lett.* **73**, 481 (1998).
- ¹⁴P. Kozodoy, J. P. Ibbetson, H. Marchand, P. T. Fini, S. Keller, J. S. Speck, S. P. Den Baars, and U. K. Mishra, *Appl. Phys. Lett.* **73**, 975 (1998).
- ¹⁵J. T. Torvik, J. I. Pankove, E. I. Iliopoulos, H. M. Ng, and T. D. Moustakas, *Appl. Phys. Lett.* **72**, 244 (1998).
- ¹⁶J. A. Freitas, Jr., O.-H. Nam, R. F. Davis, G. V. Saparin, and S. K. Obyden, *Appl. Phys. Lett.* **72**, 2990 (1998).
- ¹⁷X. Li, S. G. Bishop, and J. J. Coleman, *Appl. Phys. Lett.* **73**, 1179 (1998).
- ¹⁸F. Bertram, T. Riemann, J. Christen, A. Kaschner, A. Hoffmann, C. Thomsen, K. Hiramatsu, T. Shibata, and N. Sawaki, *Appl. Phys. Lett.* **74**, 359 (1999).
- ¹⁹J. Christen, M. Grundmann, and D. Bimberg, *J. Vac. Sci. Technol. B* **9**, 2358 (1991).
- ²⁰H. Siegle, A. Hoffmann, L. Eckey, C. Thomsen, J. Christen, F. Bertram, D. Schmidt, D. Rudloff, and K. Hiramatsu, *Appl. Phys. Lett.* **71**, 2490 (1997).
- ²¹P. Veit (private communication).
- ²²H. Siegle, G. Kaczmarczyk, L. Filippidis, A. P. Litvinchuk, A. Hoffmann, and C. Thomsen, *Phys. Rev. B* **55**, 7000 (1997).
- ²³P. Perlin, J. Camassel, W. Knap, T. Taliercio, J. C. Chervin, T. Suski, I. Grzegory, and S. Porowski, *Appl. Phys. Lett.* **67**, 2524 (1995).
- ²⁴J. Park, P. A. Grudowski, C. J. Eiting, and R. D. Dupuis, *Appl. Phys. Lett.* **73**, 333 (1998).